

NASA Technical Memorandum 102354

A Nonoscillatory, Characteristically Convected, Finite Volume Scheme for Multidimensional Convection Problems

Jeffrey W. Yokota
Sverdrup Technology, Inc.
NASA Lewis Research Center Group
Cleveland, Ohio

and

Hung T. Huynh
National Aeronautics and Space Administration
Lewis Research Center
Cleveland, Ohio

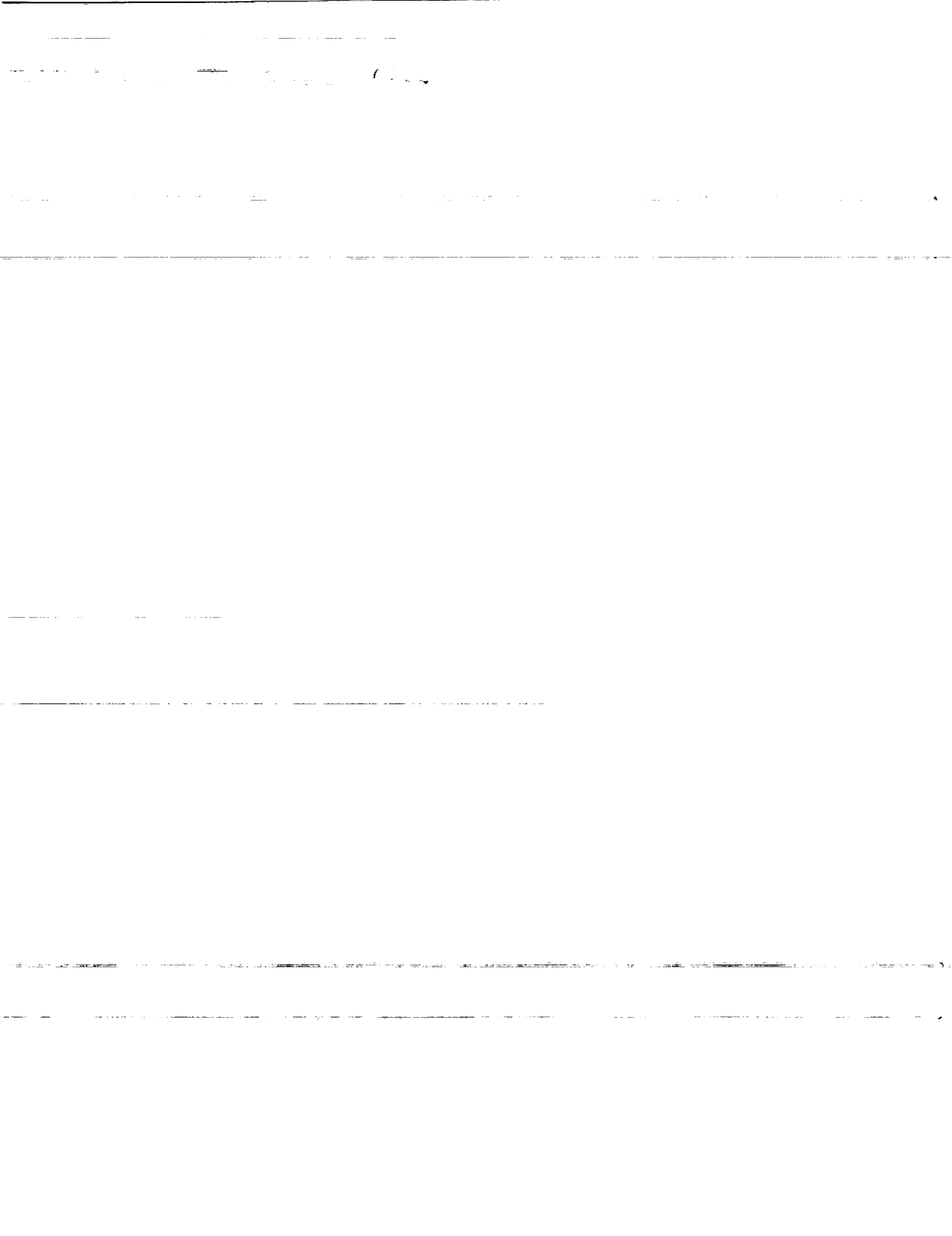
Prepared for the
28th Aerospace Sciences Meeting
sponsored by the American Institute of Aeronautics and Astronautics
Reno, Nevada, January 8-11, 1990



(NASA-TM-102354) A NONOSCILLATORY,
CHARACTERISTICALLY CONVECTED, FINITE VOLUME
SCHEME FOR MULTIDIMENSIONAL CONVECTION
PROBLEMS (NASA) 20 p CSCL 12A

N90-11497

Unclas
G3/64 0237044



A Nonoscillatory, Characteristically Convected, Finite Volume Scheme for Multidimensional Convection Problems

Jeffrey W. Yokota
Sverdrup Technology, Inc.
NASA Lewis Research Center Group
Cleveland, Ohio

Hung T. Huynh
NASA Lewis Research Center
Cleveland, Ohio

Abstract

A new, nonoscillatory upwind scheme is developed for the multidimensional convection equation. The scheme consists of an upwind, nonoscillatory interpolation of data to the surfaces of an intermediate finite volume; a characteristic convection of surface data to a midpoint time level; and a conservative time integration based on the midpoint rule. This procedure results in a convection scheme capable of resolving discontinuities neither aligned with, nor convected along, grid lines.

1. Introduction

The aerospace industry's wide acceptance of computational fluid dynamics is due mainly to the successful calculation of transonic flows.^{1,2,3} Shock capturing schemes, both upwind and central differenced, have revolutionized the way discontinuous flows are investigated.

In general it is true that an optimally tuned and gridded central differenced scheme can produce steady state solutions comparable to those produced by upwind schemes. It is equally true that upwind methods are superior in their ability to resolve unsteady flows because central differenced schemes require an artificial dissipation term that is usually tuned for steady state performance.

A number of impressive upwind methods have been developed for the one-dimensional convection equation; many of these schemes have found their way into the numerical solution of the Euler and Navier-Stokes equations.^{4,5} Most of these schemes, with the exception of a few, are second order accurate in smooth regions and first order accurate at extremas. Because this first order behavior can excessively damp unsteady calculations, methods that are uniformly second order accurate are needed.^{6,7}

In general, one-dimensional upwind schemes are only formally extended to multidimensions. The most common means of extension are the one-step Lax-Wendroff, the fractional step, and the multistep Runge-Kutta schemes, each with its own benefits and drawbacks. The one-step Lax-Wendroff scheme, while remaining conservative, requires the evaluation of cross-derivative terms whose effects on

accuracy and shock capturing have not been fully understood or exploited. The fractional step method, by far the most popular means of multidimensional extension, is not strictly time conservative, since all fluxes are not evaluated at the same time level. The multistep Runge-Kutta scheme is probably the most efficient means of extension but unfortunately suffers from an inherent dispersion error that can introduce asymmetric behavior.

The development of true multidimensional upwind schemes has only recently received the attention previously afforded to formal extensions. Davis⁸ has developed a rotated scheme that upwinds normal to shocks rather than along grid lines, while Powell and van Leer⁹ have recently formulated a convection scheme that obtains its multidimensional treatment through a residual distribution step.

The present approach, in the spirit of van Leer's MUSCL scheme,¹⁰ is to insure nonoscillatory behavior through an uniformly second order accurate nonoscillatory interpolation of data to an intermediate finite volume. A multidimensional treatment is achieved through a characteristic convection of the surface data to a midpoint time level. Strict conservation is assured through a midpoint rule time integration.

2. Analysis

To illustrate the potential difficulties associated with formally extending one-dimensional upwind concepts to higher dimensions, it is sufficient to investigate only the one-dimensional linear convection equation:

$$\frac{\partial u}{\partial t} + a \frac{\partial u}{\partial x} = 0 \quad (1)$$

The convection of various gradients (ellipse, top hat, and triangle) are solved numerically on a uniform grid, using a centered Runge-Kutta scheme with artificial dissipation, a one-step TVD Lax-Wendroff, and a multistep TVD Lax-Wendroff/Runge-Kutta scheme. Each of the gradients are constructed over a width of twenty mesh

cells and have a nondimensional amplitude of one unit and a length of one half.

Given the m-stage Runge-Kutta scheme

$$\begin{aligned} u^{(1)} &= u^n - \alpha_1 \Delta t R^n \\ u^{(2)} &= u^n - \alpha_2 \Delta t R^{(1)} \\ &\vdots \\ u^{(m)} &= u^n - \alpha_m \Delta t R^{(m-1)} \\ u^{n+1} &= u^{(m)} \end{aligned} \quad (2)$$

where $\alpha_1, \alpha_2, \text{etc.}$ are scalar constants and Δt is the time step. The spatial difference term

$$R = \frac{\partial u}{\partial x} \approx (u_{i+1/2} - u_{i-1/2}) / \Delta x \quad (3)$$

can be constructed from a central difference approximation with an added nonlinear artificial dissipation term² or a flux limited approximation

$$u_{i+1/2} = u_i + 0.5 \phi_i \Delta^+ u_i \quad (4)$$

where the convection speed $a > 0$ is constant; Δ^+ is a first order forward difference operator; and ϕ_i is the TVD limiter chosen, most often, to take one of the following forms

$$\begin{aligned} \phi &= \frac{|r| + r}{1 + r} \\ \phi &= \max(0, \min(r, 1)) \\ \phi &= \max(0, \min(2r, 1), \min(r, 2)) \\ \phi &= \max(0, \frac{2^n r}{(1 + |r|^{1/n})^n}) \\ r &= \frac{\Delta^+ u_{i-1}}{\Delta^+ u_i} \end{aligned} \quad (5)$$

corresponding to van Leer's¹¹ continuous; Roe's¹² Minmod and Superbee; and Liou's¹³ exponential limiters, respectively.

These limiters are also used in the construction of Sweby's¹⁴ second-order TVD Lax-Wendroff formulation

$$u_i^{n+1} = u_i^n - \nu \Delta^- u_i - 0.5 \Delta^- \phi (1 - \nu) \nu \Delta^+ u_i \quad (6)$$

where $\nu = a \Delta t / \Delta x$ and Δ^- is a first order backward difference operator.

To investigate the performance of these schemes, a number of test calculations were performed for eighty time steps at a Courant number of one half. The results from a second order, centered, four stage Runge-Kutta scheme are clearly oscillatory (Fig. 1) and may be deemed inappropriate for unsteady calculations. It may be conjectured that

a time dependent artificial dissipation term could improve this behavior, but at present no such treatment exists.

Results from the one-step TVD Lax-Wendroff method (Figs. 2-4) are superior to those obtained from the centered scheme and illustrate the relative advantages of the upwind method.

A popular means of extending these TVD concepts to higher dimensions is through a multistep scheme, which unfortunately can introduce undesirable errors. Figures 5 and 6 show that asymmetry and oscillation can be introduced even into the one dimensional problem and thus a formal extension to higher dimensions may be ill advised.

The asymmetry produced by the Runge-Kutta scheme occurs because of the effective limiter created by the multi-step formulation. The use of an identical symmetric limiter in each of the multiple steps does not insure an overall symmetric behavior. The multi-stage formulation has the effect of generating nonlinear, spatially shifted terms of the form $\phi_i \phi_{i-1}$, which can no longer guarantee a symmetric behavior. The use of different limiters in each step would be an obvious way of addressing this asymmetry and would introduce, in effect, MacCormack's¹⁵ predictor-corrector philosophy.

The multi-step formulation can also degrade, with respect to the results from the one-step scheme, the performance of the flux limiters. Liou's exponential limiter, which performs well in the one-step scheme, can be rendered non-TVD and oscillatory in the multi-step formulation. This occurs because the exponential limiter is TVD for

$$r \leq \frac{1}{(2^{(n-1)/n} - 1)^n} \quad (7)$$

which is unconditionally true only for $n = 1$. As n increases, the limiter has the desirable behavior of becoming less diffusive but also produces a more restrictive TVD condition. While this condition seems not to be violated in the one-step scheme, it is in fact compromised in the first step of the multi-step formulation, thus allowing oscillations to develop. It again becomes clear that formal extensions to higher dimensions may be ill advised.

Despite the successes achieved in one-dimension, the development of the 'ultimate' convection scheme has proven elusive. Goodman and LeVeque¹⁶ have shown that the desire for accuracy higher than first order requires sacrificing the TVD property in two-dimensions. The obvious next step is to retain a nonoscillatory behavior despite losing the TVD property. This is the rationale taken for uniformly second order accurate nonoscillatory one-dimensional methods.

To illustrate the difficulties associated with the development of multidimensional schemes, the following categories are defined:

1) Omnidirectionally Nonoscillatory: No new extremas are created in any arbitrary direction.

2) Preferred Direction Nonoscillatory: No new extremas are created in a preferred direction.

3) Grid Aligned Nonoscillatory: No new extremas are created along at least one grid direction.

Most present day nonoscillatory schemes meet the requirements of grid aligned nonoscillatory behavior, while Davis's⁸ rotated scheme satisfies the definition of preferred direction nonoscillation. Definitions 2 and 3 are necessary but not sufficient conditions for an omnidirectional nonoscillatory behavior, which is in fact unlikely to be satisfied by anything less than the convection of the exact solution. This seemingly bold statement can be illustrated by a one-dimensional convection of a two-dimensional distribution where dissipation along the convection direction can create new extremas in the cross stream direction. A variation of Zalesak's¹⁷ notched cylinder problem can be used to illustrate this point. A notch, fourteen mesh cells wide and twenty mesh cells deep, is cut out of a thirty mesh cell diameter cylinder 0.75 unit wide and 0.5 unit high. This distribution, Fig.7, can be convected (forty time steps at a Courant number of one half, on a uniform grid) along the notch's length-wise direction by a simple first-order upwind scheme. The two-dimensional distribution uncouples into a series of one-dimensional problems, each of which undergoes some amount of amplitude damping. Since the distribution is two-dimensional and no information is passed in the cross convection direction, the amplitude damping cannot be applied uniformly and thus oscillations are created in the cross-convection direction, Fig.8. As a result, it would seem that even a first order TVD scheme could be oscillatory in multidimensions, indicating that the strict nonoscillatory property is more restrictive than the TVD property, which is the opposite of what is known to be true in one-dimension. Based on this observation, one might come to the conclusion that, since anything less than an exact solution cannot guarantee nonoscillation, there is little to be gained by trying to develop a truly multidimensional formulation. However, this conclusion would be short sighted, since one could still make significant improvements in the accuracy of unsteady calculations without having to satisfy the strict nonoscillatory properties of definition 1. In other words, the nonoscillatory property, like the TVD property, is not the only measure of accuracy and may have to be sacrificed, at least in practice, by some other, yet to be established, definition of 'goodness'.

3. Two-Dimensional Formulation

Consider the two-dimensional linear convection equation:

$$\frac{\partial u}{\partial t} + a \frac{\partial u}{\partial x} + b \frac{\partial u}{\partial y} = 0 \quad (8)$$

where

$$a = a(y) \quad \text{and} \quad b = b(x)$$

This equation can be solved numerically, on a uniform grid, by a scheme that interpolates grid point data to the surfaces of an intermediate finite volume; characteristically convects the surface data to a midpoint time level; and updates the solution with a midpoint rule time integration.

To insure the production of a nonoscillatory solution, at least directionally, face values must be constructed in a nonoscillatory manner. To avoid excessive amounts of damping, this interpolation must be at least uniformly second order accurate.

A second order accurate, nonoscillatory interpolation, which relies heavily upon a geometric interpretation of the standard TVD concepts, has been recently developed.⁷ A one-dimensional interpolation for a positive convection speed can be written:

$$u_{i+1/2} = u_i + S_i \Delta x / 2 \quad (9)$$

where S_i is the slope of a piecewise linear distribution of data over the intermediate finite volume around each grid point. The slope associated with the Minmod¹² scheme can be defined as the median of the slopes corresponding to first order upwinding, central differencing, and second order Warming-Beam upwinding. Thus the Minmod slope is

$$S_i^{Minmod} = \frac{Median(0, u_{i+1/2}^c - u_i, u_i - u_{i-1/2}^c)}{\Delta x / 2} \quad (10)$$

where

$$u_{i+1/2}^c = 0.5(u_i + u_{i+1}) \quad (11)$$

while the slope corresponding to Roe's Superbee¹² scheme can be interpreted as:

$$S_i^{Superbee} = \frac{Median \left(\begin{array}{c} 0, u_{i+1/2}^c - u_i, \\ u_i - u_{i-1/2}^c, \\ u_i - u_{i-1}, u_{i+1} - u_i \end{array} \right)}{\Delta x / 2} \quad (12)$$

These schemes are second order accurate in smooth regions and first order accurate at extrema. To remove this first order behavior, Harten and Osher⁶ developed the uniformly second order accurate UNO2 scheme. This scheme can be written as the Minmod slope described above, but with a $u_{i+1/2}^c$ value obtained from a nonoscillatory quadratic interpolation:

$$u_{i+1/2}^c = 0.5(u_i + u_{i+1}) - 0.25D_{i+1/2} \quad (13)$$

where

$$D_{i+1/2} = \text{minmod}(D_i, D_{i+1}) \quad (14)$$

$$D_i = D_{i+1} - 2D_i + D_{i-1}$$

and

$$\begin{aligned} \text{minmod}(a, b) = \\ \text{sign}(a)\text{max}(0, \text{sign}(ab)\text{min}(|a|, |b|)) \end{aligned} \quad (15)$$

This geometric redefinition is rich in extensions and has led to the development of Huynh's SONIC schemes.⁷ By incorporating this new definition of $u_{i+1/2}^c$ into the Superbee slope, one can produce Huynh's uniformly second order accurate SONIC-B scheme, which is less dissipative than the UNO2 scheme. A further extension can be achieved by first defining the slope:

$$S_i^\phi = \frac{u_{i+1/2}^c - u_{i-1/2}^c}{\Delta x} \quad (16)$$

and then using this value to construct a new slope:

$$S_i^{\text{SONIC-A}} = \text{Median}(0, S_i^\phi, S^{\text{SONIC-B}}) \quad (17)$$

This modification results in the SONIC-A scheme, which is also uniformly second order accurate but less overcompressive than the SONIC-B scheme.⁷

The median of three quantities, required in the sonic interpolations, is evaluated as follows

$$\begin{aligned} \text{median}(x_1, x_2, x_3) = x_1 \\ + \text{minmod}(x_2 - x_1, x_3 - x_1) \end{aligned} \quad (18)$$

while the median of five quantities is evaluated as

$$\text{median}(x_1, x_2, x_3, x_4, x_5) = \text{median}(X_1, X_2, x_5) \quad (19)$$

where

$$\begin{aligned} X_1 &= \text{median}(x_1, x_2, x_3) \\ X_2 &= x_1 + x_2 + x_3 + x_4 \\ &\quad - \text{max}(x_1, x_2, x_3, x_4) \\ &\quad - \text{min}(x_1, x_2, x_3, x_4) - X_1 \end{aligned}$$

The SONIC interpolations are used in each direction to construct surface data from the grid point values at time level n . The surface data is then advanced to a midpoint time level using a characteristic convection, which is based on a bilinear distribution

of data over a quarter of the intermediate finite volume.

At time level $n + 1/2$, the surface data is evaluated by first following the characteristic back to its spatial location at time level n and then by constructing its value from a bilinear distribution over the corresponding quadrant's corner values. These quadrant values correspond to the intermediate cell's centered, face, and corner values. For positive convection speeds a and b , the surface data at time level $n + 1/2$ can be evaluated as:

$$\begin{aligned} u_{i+1/2,j}^{n+1/2} = & u_{i+1/2,j}^n - \frac{a\Delta t}{\Delta x}(u_{i+1/2,j}^n - u_{i,j}^n) \\ & - \frac{b\Delta t}{\Delta y}(u_{i+1/2,j}^n - u_{i+1/2,j-1/2}^n) \\ & + \frac{ab\Delta t^2}{\Delta y\Delta x}(u_{i+1/2,j}^n - u_{i+1/2,j-1/2}^n \\ & - u_{i,j}^n + u_{i,j-1/2}^n) \end{aligned} \quad (20)$$

where the corner value

$$u_{i+1/2,j-1/2}^n = 0.5(I_x I_y + I_y I_x) u_{i,j}^n \quad (21)$$

is evaluated as a symmetric product of I_x and I_y , the one dimensional sonic interpolation operators in the x and y directions, respectively.

Once the surface data has been convected to the time level $n + 1/2$, the finite volume fluxes are evaluated and the values at the grid points are updated by the midpoint rule:

$$\begin{aligned} u_{i,j}^{n+1} = & u_{i,j}^n - \Delta t \left(\frac{F_{i+1/2,j}^{n+1/2} - F_{i-1/2,j}^{n+1/2}}{\Delta x} \right. \\ & \left. + \frac{G_{i,j+1/2}^{n+1/2} - G_{i,j-1/2}^{n+1/2}}{\Delta y} \right) \end{aligned} \quad (22)$$

where $F = au$ and $G = bu$.

4. Results

A series of two-dimensional convection problems are used to illustrate the scheme's ability to resolve discontinuities that are neither aligned with, nor convected along, grid lines.

Numerical results are obtained for the convection of a cone, box, and cylinder along arbitrary flow directions of 0, 45, and 70 degrees. Calculations were performed on a uniform grid of 100x100 mesh cells for 100 time steps at a Courant number of one half. Both the cone and cylinder have a 10 mesh cell radius of 0.25 unit long and are 4 units high. The box has a 20 mesh cell square base of 0.5 unit wide and is also 4 units high. The numerical

results using the SONIC-A interpolation, Figures 9 to 20, show that the various corner, edge, and peak discontinuities can be resolved for various flow angles. The sharp edges associated with the box and cylinder distributions are smoothed over a couple of mesh cells while the magnitude of the cone's peak is reduced by about six to ten percent. This damping, while not unexpected, has been kept to a minimum on this relatively coarse grid. These calculations are also nonoscillatory in that no trailing, leading, or image oscillations are observed in any of these test cases.

Results for the more difficult case of a rotating cone and cutout cylinder,¹⁸ Fig. 21, are also included to demonstrate the scheme's shock capturing capabilities. Calculations were performed on a uniform 100x100 mesh cell grid using the Minmod, Superbee, SONIC-B, and SONIC-A interpolations. Both the cone and the cylinder distributions have a 30 mesh cell diameter of 0.75 unit wide and an amplitude of 0.5 unit high. The cylinder's notch is 6 mesh cells wide and 24 mesh cells deep. The center of rotation is located at the grid center point, P(50,50), while the cone is located at P(25,50) and the cylinder is centered at P(75,50). These calculations were run for one and six complete rotations, which correspond to 628 and 3768 time steps, respectively. This solid body rotation, characterized by the velocity field

$$\begin{aligned}
 a(y) &= -(y - y_0)\omega \\
 b(x) &= (x - x_0)\omega \\
 x_0 &= x(50, 50) \\
 y_0 &= y(50, 50) \\
 \omega &= 0.1
 \end{aligned}
 \tag{23}$$

is an extremely difficult test case since the Courant number, dispersion, and damping errors vary in magnitude throughout the domain, making the symmetric resolution of a symmetric problem highly unlikely.

After one complete rotation, the discontinuities are captured extremely well by the Superbee, SONIC-B, and SONIC-A interpolations. The Minmod results, Fig.22, are extremely dissipative and retain only the gross features of the initial distributions. The Superbee calculation, Fig.23, resolves the notched cylinder well but shows a slight overcompression of the cone distribution. The SONIC-B interpolation, Fig.24, results in a non-TVD steepening of the notched cylinder's narrow bridge but has not overcompressed the cone. The SONIC-A interpolation produces the best overall results, Fig.25, since the discontinuities are captured without an excessive amount of overcompression or damping.

The results after six complete revolutions are somewhat less encouraging. The Minmod calculation, Fig.26, has all but caused the distributions

to disappear. The Superbee interpolation, Fig.27, again captures the notched cylinder extremely well but compresses the cone into a cylindrical shape. The SONIC-B results, Fig.28, are slightly less overcompressive than the Superbee calculation, but are asymmetric in form. The SONIC-A results are greatly damped and no longer retain the cylinder's plateau region (Fig.29). However, the cone distribution, albeit dissipated, still retains much of its original shape.

The performance of the SONIC-A interpolation is the most desirable from the standpoint of being able to retain the overall shapes of the original distributions. Since the SONIC-A interpolation is not overcompressive, it does not transform gentle gradients into steep ones, and thus retains the most important features of the original distributions.

5. Concluding Remarks

A new upwind scheme, based on a uniformly second order accurate nonoscillatory interpolation, is developed for the multidimensional convection equation. Numerical results illustrate the scheme's ability to resolve, without excessive amounts of dispersion or damping errors, discontinuities neither aligned with, nor convected along, grid lines.

It is suggested that the strict nonoscillatory property in multidimensions is unlikely to be satisfied by anything less than the convection of the exact solution and is more restrictive than the TVD property. If one accepts this belief, it then becomes obvious that a more practical definition of 'goodness' is needed for multidimensional problems.

6. Acknowledgments

The first author would like to acknowledge a number of helpful conversations with Dr. Eli Turkel and Dr. Ken Powell. The development of a characteristic-like scheme was first proposed by Dr. Turkel, while Dr. Powell was kind enough to share some of his experiences with multidimensional convection.

7. References

- [1] Jameson, A., and Caughey, D.A., "A Finite-Volume Method for Transonic Potential Flow Calculations," Proceedings of the AIAA 3rd Computational Fluid Dynamics Conference, pp. 35-54, Albuquerque, N.M., June 1977.
- [2] Jameson, A., "Transonic Flow Calculations for Aircraft," in *Lecture Notes in Mathematics*, Brezzi, F., ed., vol. 1127, pp. 156-242, Springer-Verlag, New York, 1985.
- [3] Pulliam, T.H., "Implicit Finite-Difference Methods for the Euler Equations,"

- in *Advances in Computational Transonics, Recent Advances in Numerical Methods in Fluids*, ed. Habashi, W.G., vol 4, pp. 503-575, Pineridge Press, Swansea, U.K., 1985.
- [4] Yee, H., "Construction of Explicit and Implicit Symmetric TVD Schemes and their Applications," *Journal of Computational Physics*, vol 68, pp. 151-179, 1987.
- [5] Anderson, W.K., Thomas, J.L., and Whitfield, D.L., "Multigrid Acceleration of the Flux Split Euler Equations," AIAA Paper 86-0274, January 1986.
- [6] Harten, A., and Osher, S., "Uniformly Higher-Order Accurate Nonoscillatory Schemes I," *SIAM Journal of Numerical Analysis*, vol 24, pp. 279-309, 1987.
- [7] Huynh, H.T., "Second-Order Accurate Nonoscillatory Schemes for Scalar Conservation Laws," 6th International Conference on Numerical Methods in Laminar and Turbulent Flow, Swansea, U.K., July 1989.
- [8] Davis, S.F., "A Rotationally-Biased Upwind Difference scheme for the Euler Equations," *Journal of Computational Physics*, vol 56, 1984.
- [9] Powell, K.G., and van Leer, B., "A Genuinely Multi-Dimensional Upwind Cell-Vertex Scheme for the Euler Equations," AIAA Paper 89-0095, 27 Aerospace Sciences Meeting, Reno, Nevada, January 1989.
- [10] van Leer, B., "Towards the Ultimate Conservative Difference Scheme. V, A Second Order Sequel to Godunov's Method," *Journal of Computational Physics*, vol. 32, pp. 101-136, 1979.
- [11] van Leer, B., "Towards the Ultimate Conservative Difference Scheme. II, Monotonicity and Conservation Combined in a Second-Order Scheme," *Journal of Computational Physics*, vol 14, pp. 361-370, 1974.
- [12] Roe, P.L., "Some Contributions to the Modelling of Discontinuous Flows," *Lectures in Applied Mathematics*, vol. 22, pp. 163-193, 1985.
- [13] Liou, M.S., and Hsu, A.T., "A Time Accurate Finite Volume High Resolution Scheme for the Three Dimensional Navier-Stokes Equations," AIAA Paper 89-1994, Proceedings of the 9th Computational Fluid Dynamics Conference, Buffalo, N.Y., June 1989.
- [14] Sweby, P.K., "High Resolution Schemes using Flux Limiters for Hyperbolic Conservation Laws," *SIAM Journal of Numerical Analysis*, vol 21, pp. 995-1011, 1984.
- [15] MacCormack, R.W., "The Effect of Viscosity in Hypervelocity Impact Cratering," AIAA Paper 69-354, 1969.
- [16] Goodman, J.B., and LeVeque, R.J., "On the Accuracy of Stable Schemes for 2D Conservation Laws," *Mathematics of Computation*, vol. 45, pp. 15-21, July 1985.
- [17] Zalesak, S.T., "Fully Multidimensional Flux-Corrected Transport Algorithms for Fluids," *Journal of Computational Physics*, vol. 31, pp. 335-362, 1979.
- [18] Muns, C.D., "On the Numerical Dissipation of High Resolution Schemes for Hyperbolic Conservation Laws," *Journal of Computational Physics*, vol. 77, pp. 18-39, 1988.

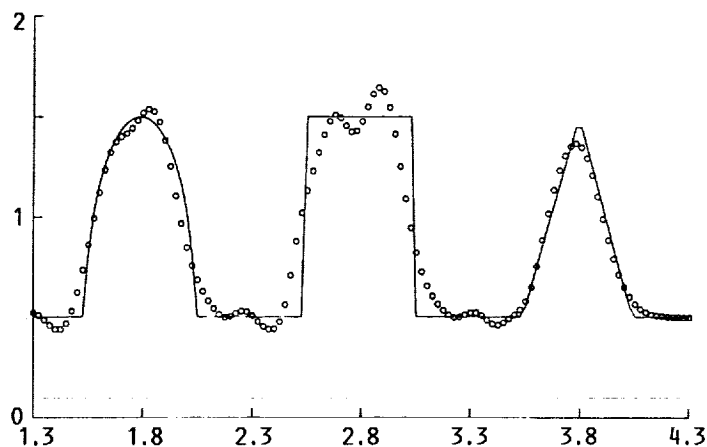


FIGURE 1. - CENTERED 4-STAGE RUNGA-KUTTA CALCULATION.

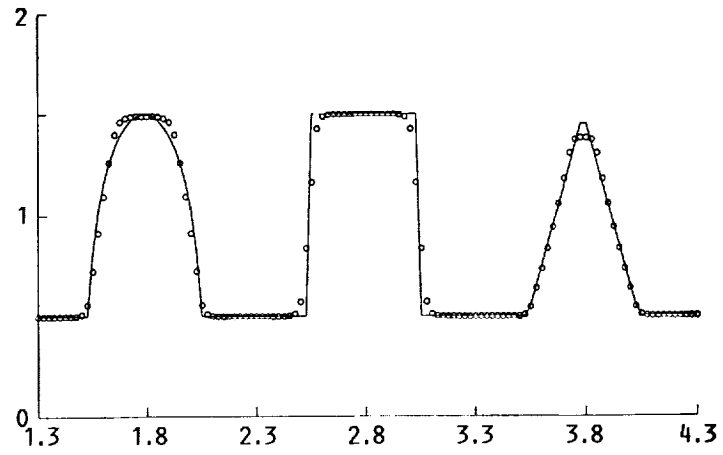


FIGURE 2. - 1-STEP LAX-WENDROFF WITH SUPERBEE LIMITER.

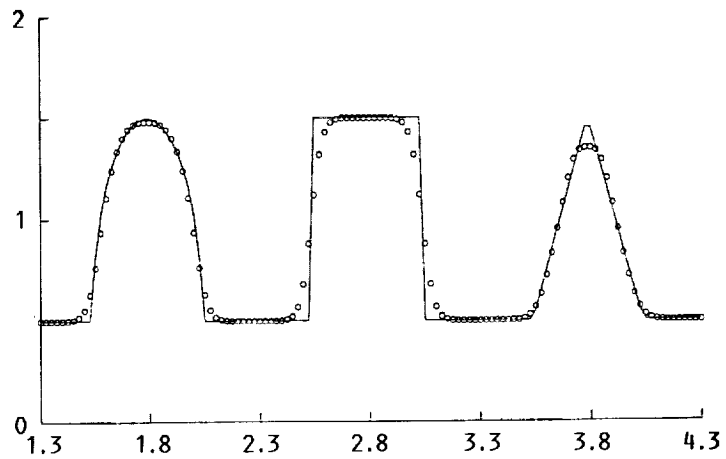


FIGURE 3. - 1-STEP LAX-WENDROFF WITH VAN LEER'S LIMITER.

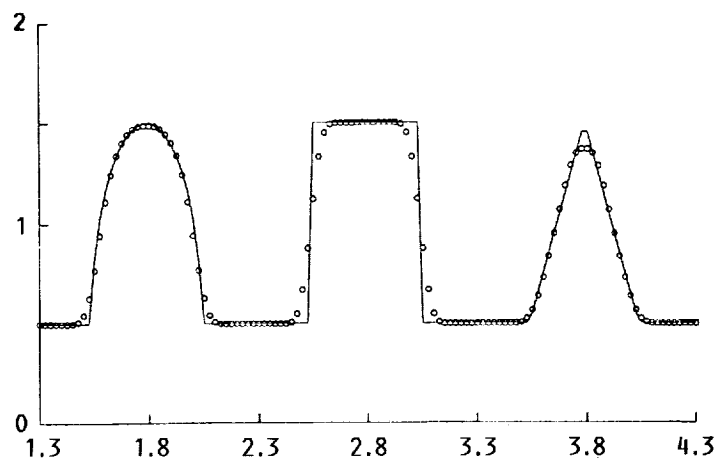


FIGURE 4. - 1-STEP LAX-WENDROFF WITH LIOU'S EXPONENTIAL LIMITER, $N = 10$.

ORIGINAL PAGE
BLACK AND WHITE PHOTOGRAPH

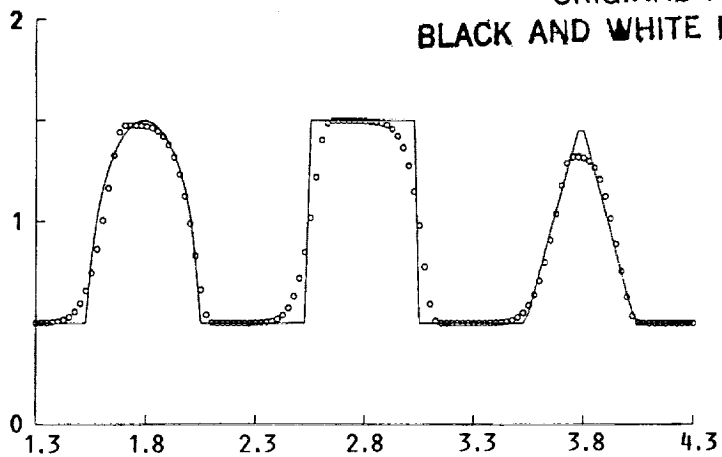


FIGURE 5. - 2-STEP LAX-WENDROFF WITH VAN LEER'S
LIMITER.

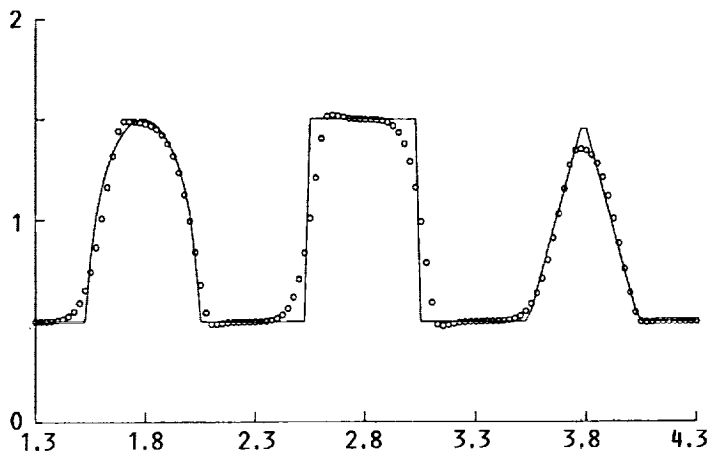


FIGURE 6. - 2-STEP LAX-WENDROFF WITH LIOU'S EXPONENTIAL
LIMITER, $N = 10$.

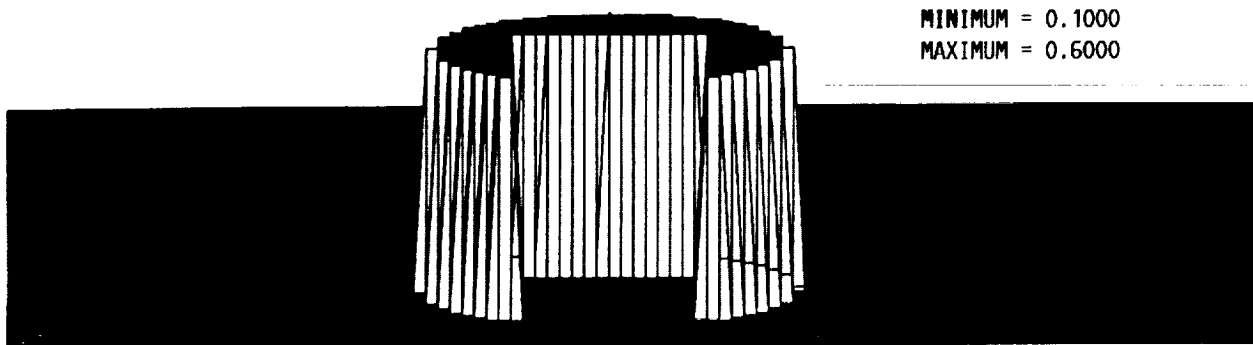


FIGURE 7. - INITIAL CONDITION - 1-D CONVECTION.

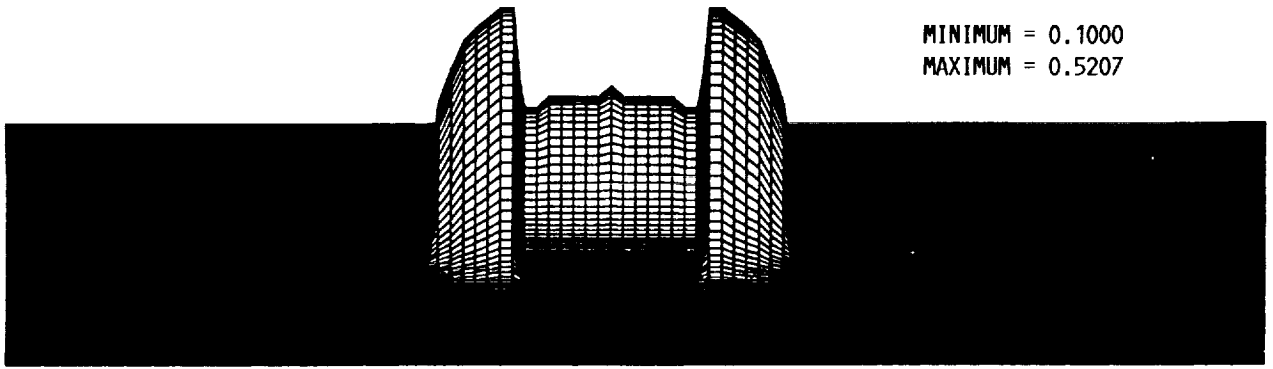


FIGURE 8. - 1-D CONVECTION OF THE 2-D DISTRIBUTION.



FIGURE 9. - INITIAL CONDITION: CONE.

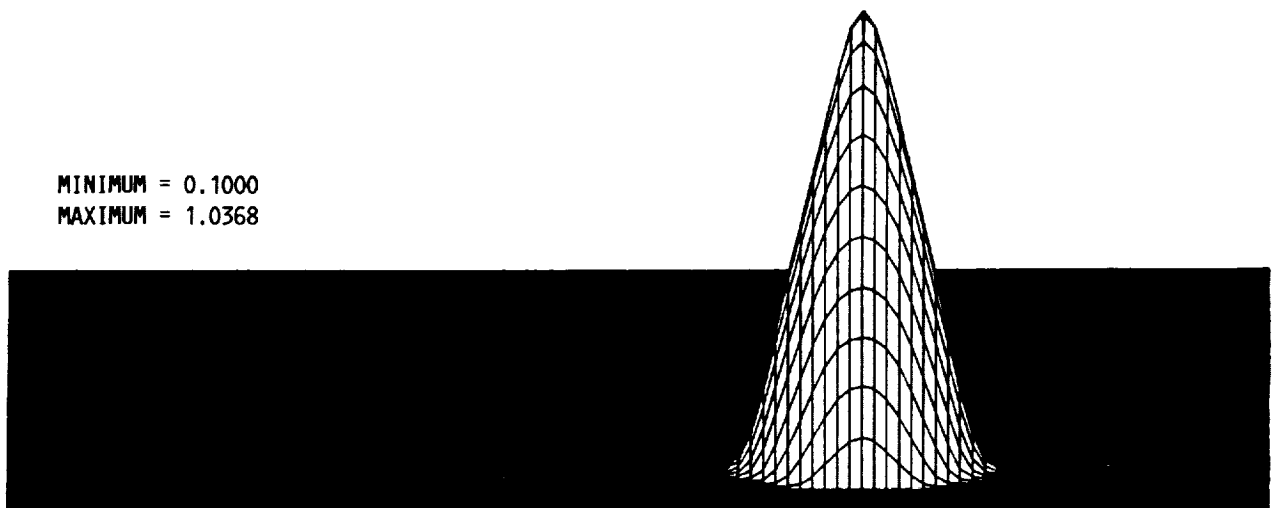


FIGURE 10. - 0 DEGREE CONVECTION - CONE.

ORIGINAL PAGE
BLACK AND WHITE PHOTOGRAPH

MINIMUM = 0.1000
MAXIMUM = 0.9964

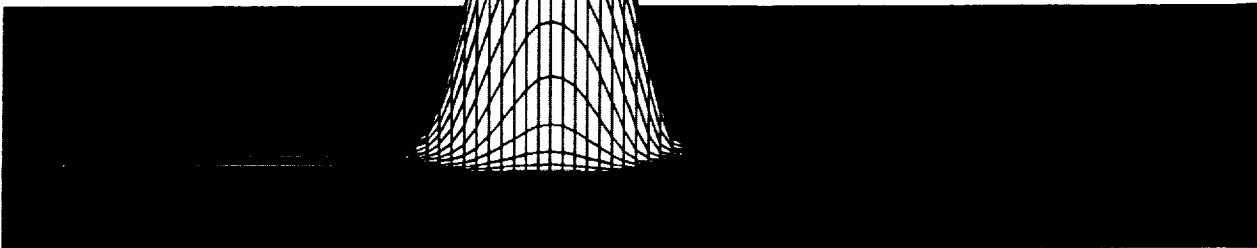


FIGURE 11. - 45 DEGREE CONVECTION - CONE.

MINIMUM = 0.1000
MAXIMUM = 0.9987



FIGURE 12. - 70 DEGREE CONVECTION - CONE.

ORIGINAL PAGE
BLACK AND WHITE PHOTOGRAPH

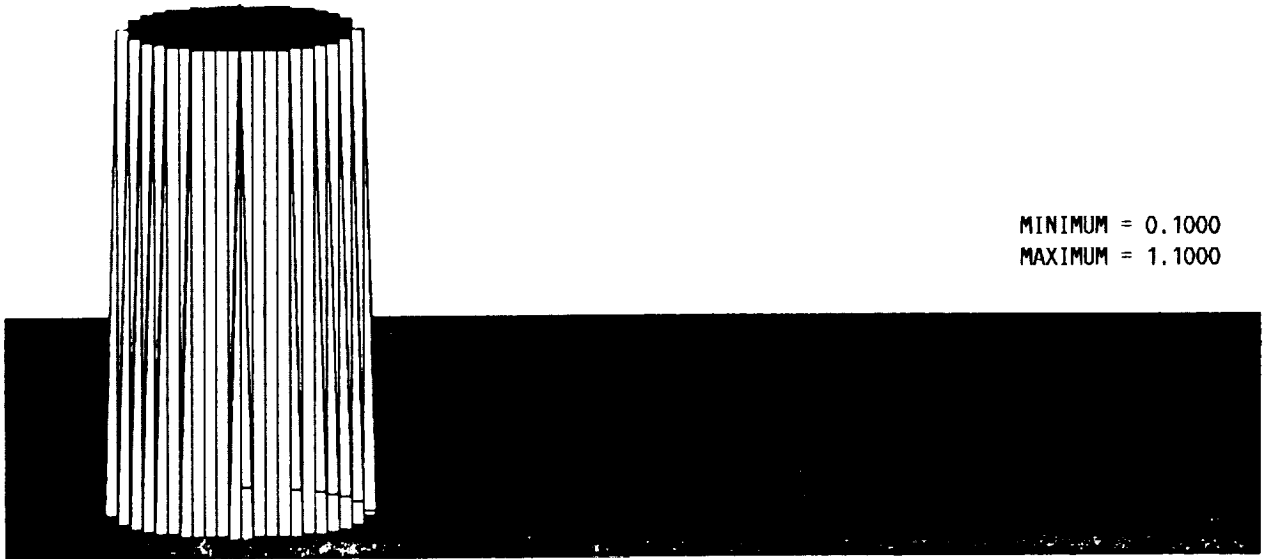


FIGURE 13. - INITIAL CONDITION - CYLINDER.

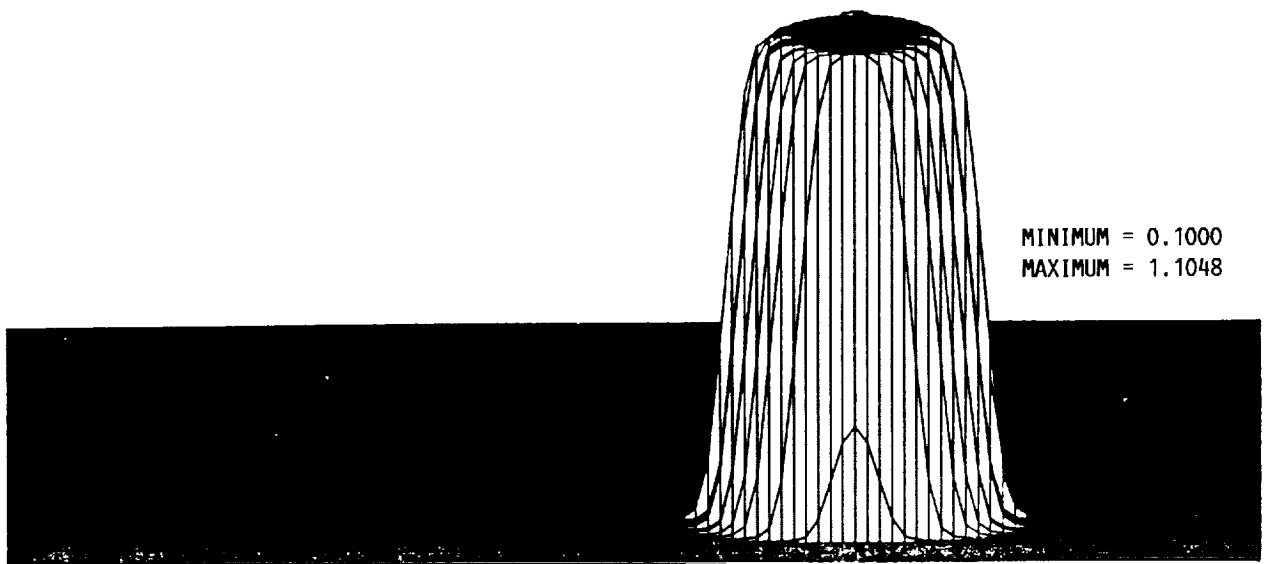


FIGURE 14. - 0 DEGREE CONVECTION - CYLINDER.

ORIGINAL PAGE
BLACK AND WHITE PHOTOGRAPH

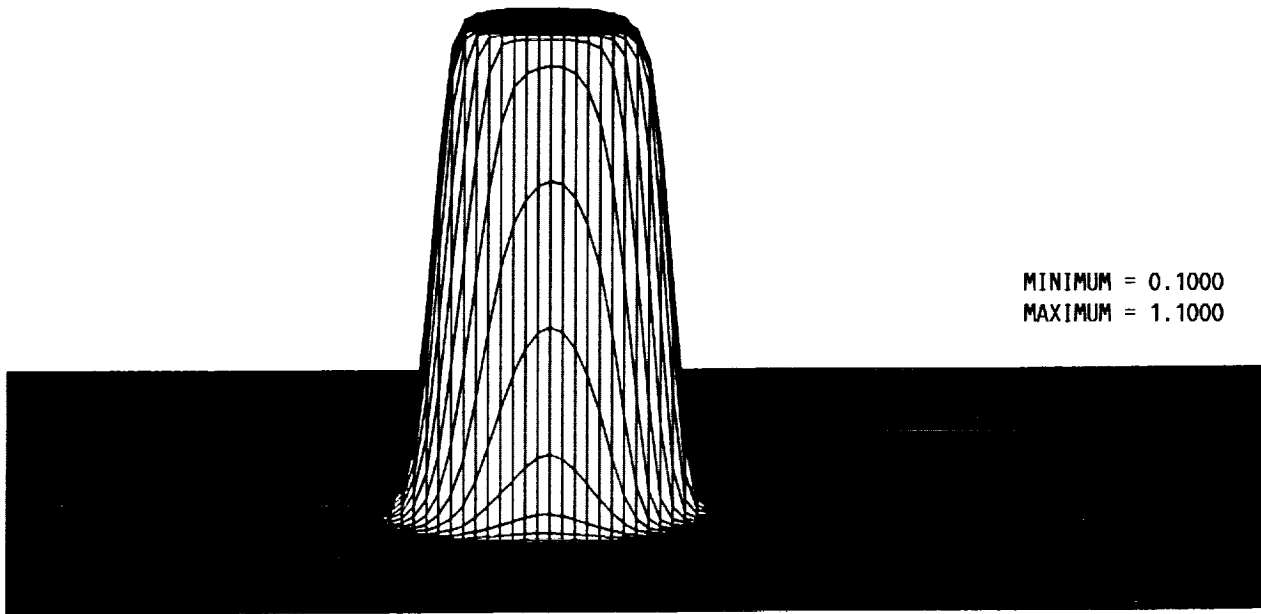


FIGURE 15. - 45 DEGREE CONVECTION - CYLINDER.

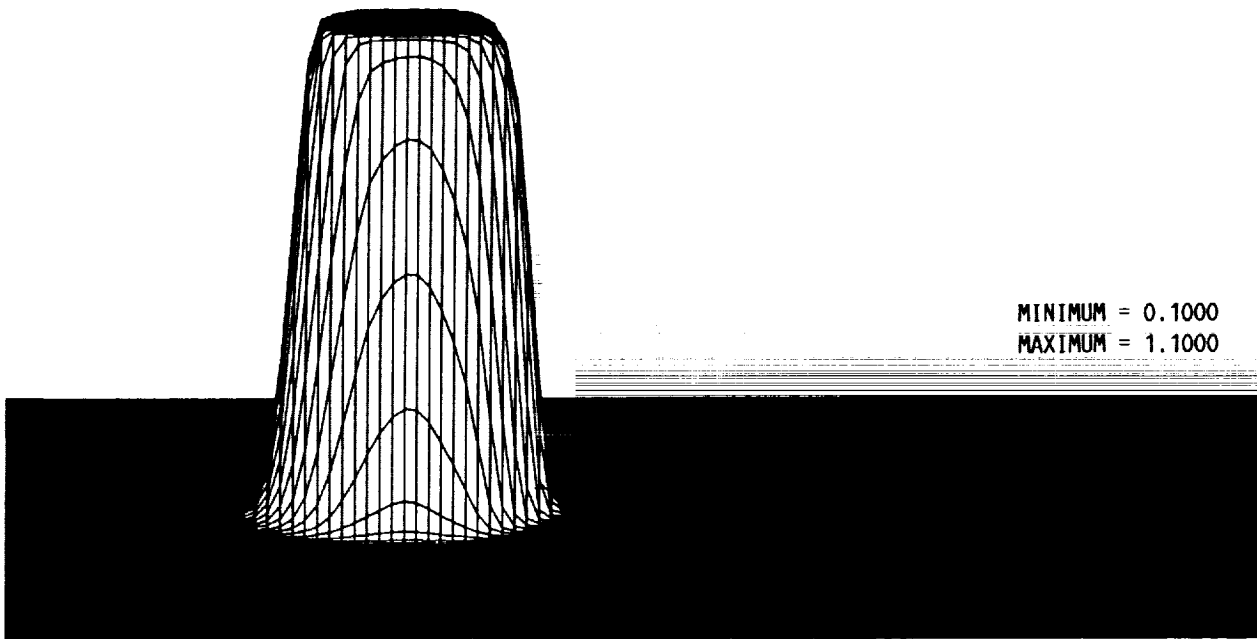


FIGURE 16. - 70 DEGREE CONVECTION - CYLINDER.

ORIGINAL PAGE
BLACK AND WHITE PHOTOGRAPH

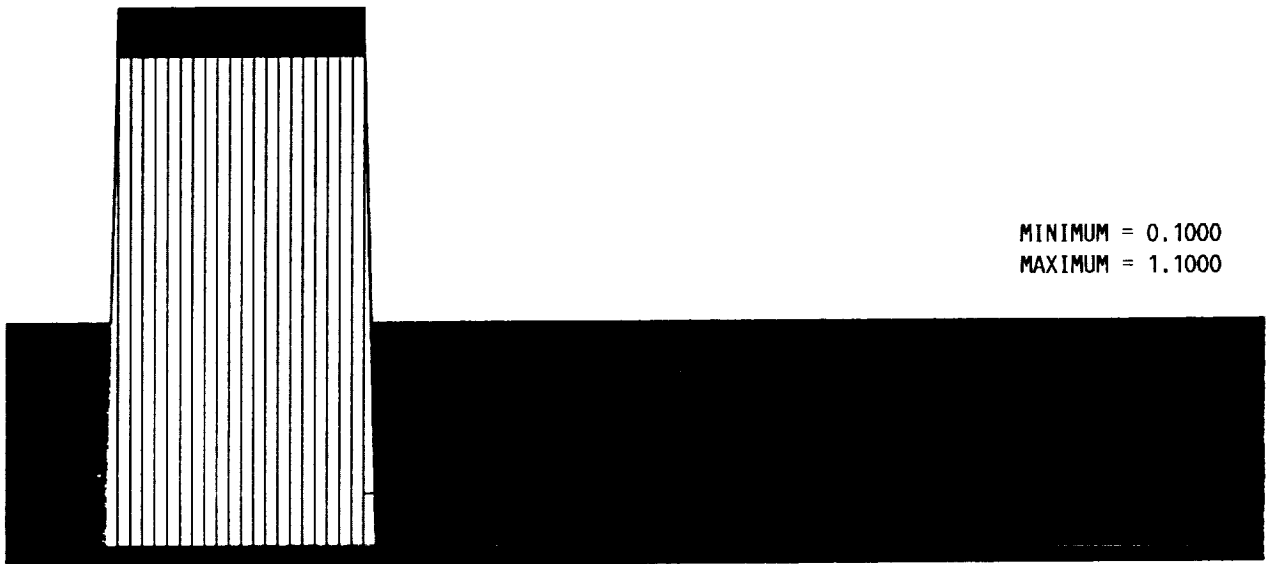


FIGURE 17. - INITIAL CONDITION - BOX.

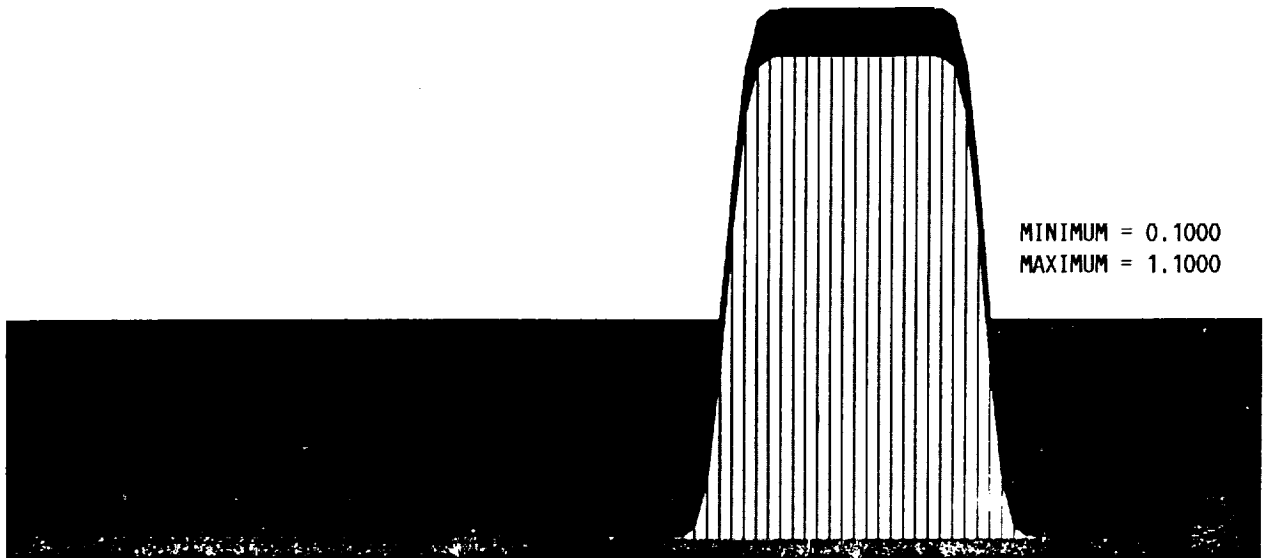


FIGURE 18. - 0 DEGREE CONVECTION - BOX.

ORIGINAL PAGE
BLACK AND WHITE PHOTOGRAPH

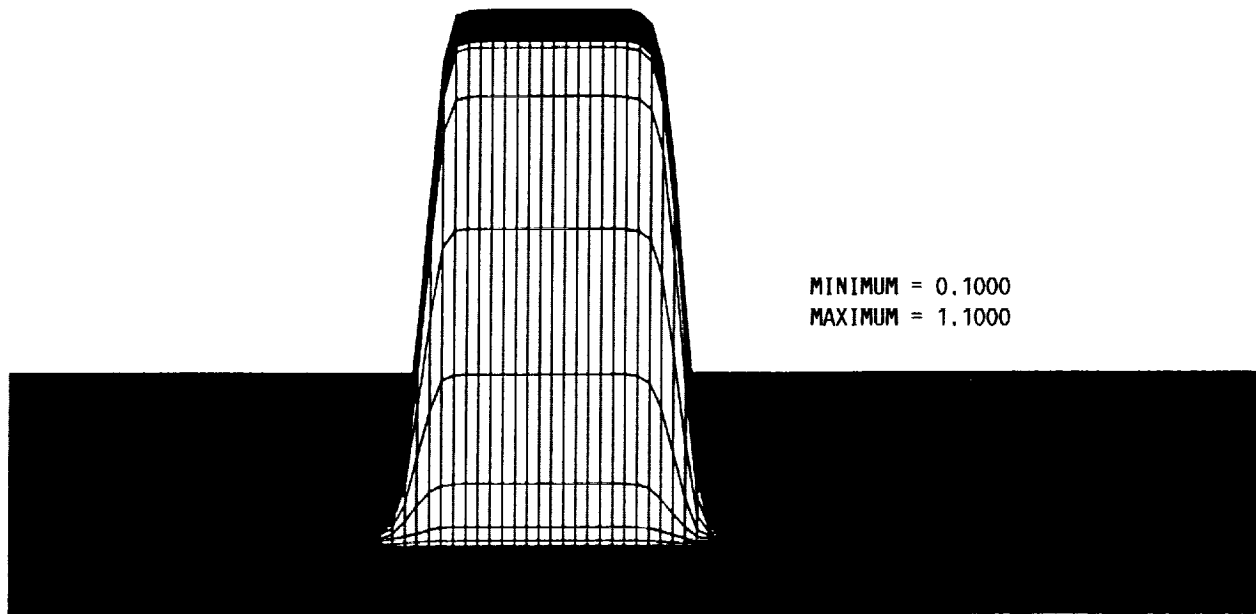


FIGURE 19. - 45 DEGREE CONVECTION - BOX.

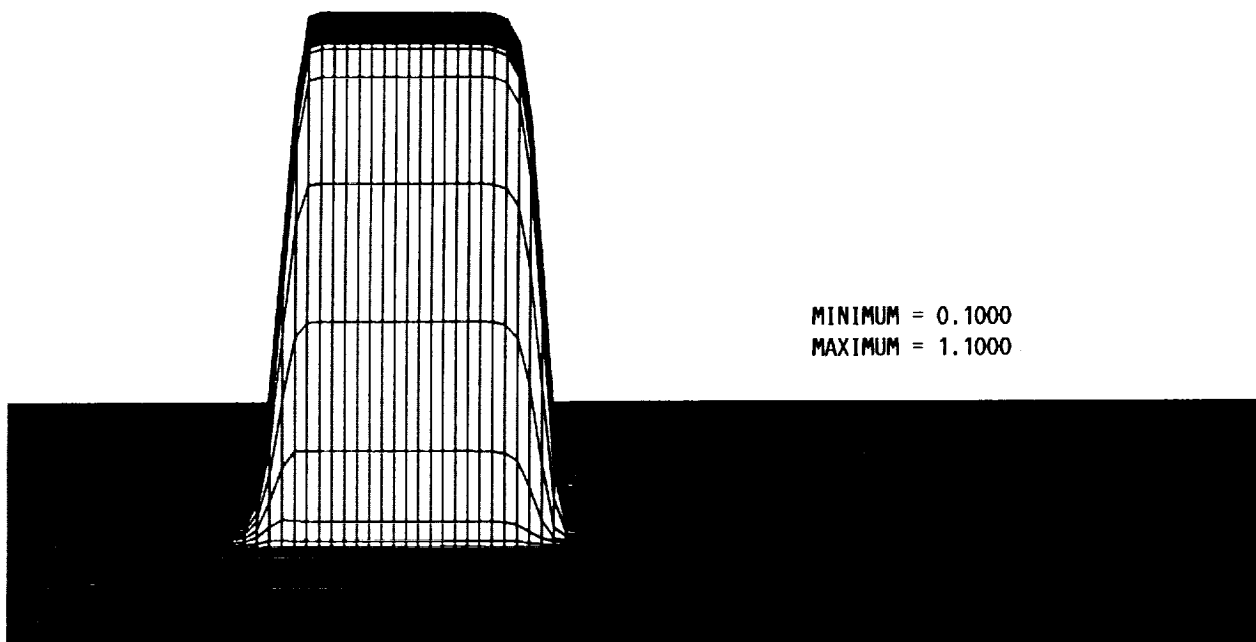


FIGURE 20. - 70 DEGREE CONVECTION - BOX.

ORIGINAL PAGE
BLACK AND WHITE PHOTOGRAPH

MINIMUM = 0.1000
MAXIMUM = 0.5000

MINIMUM = 0.1000
MAXIMUM = 0.5000

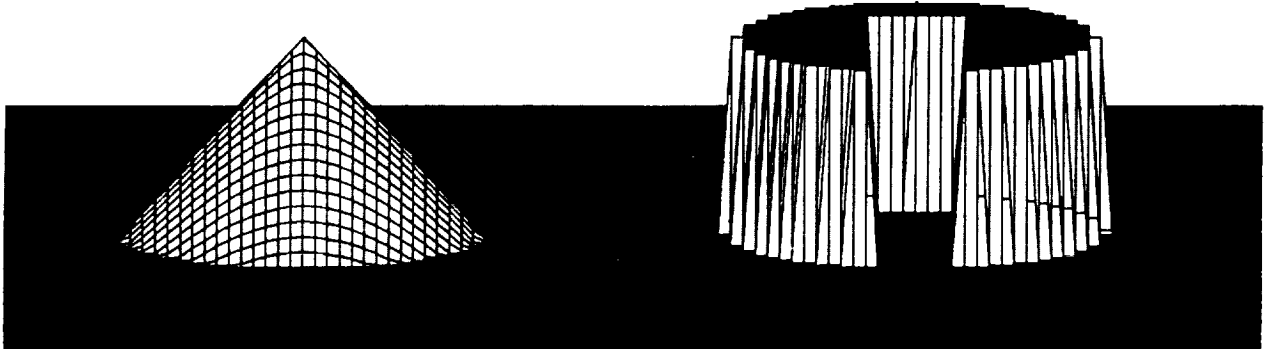


FIGURE 21. - INITIAL CONDITION - SOLID BODY ROTATION.

MINIMUM = 0.1000
MAXIMUM = 0.3715

MINIMUM = 0.1000
MAXIMUM = 0.4605

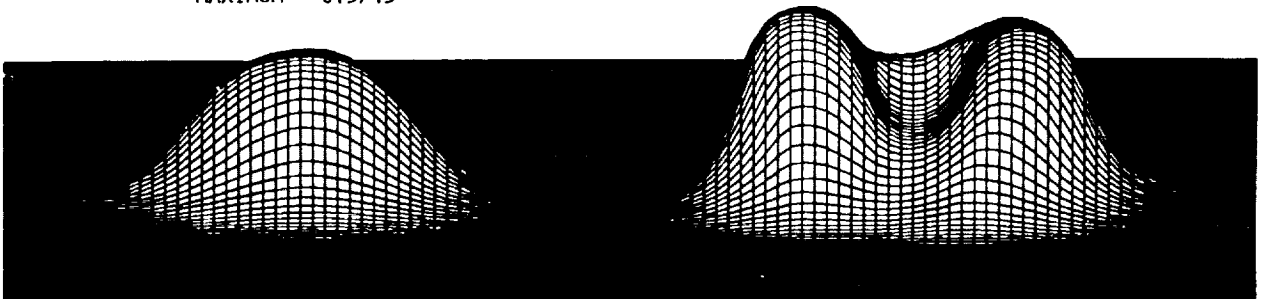


FIGURE 22. - 1 ROTATION - MINMOD INTERPOLATION.

ORIGINAL PAGE
BLACK AND WHITE PHOTOGRAPH

MINIMUM = 0.1000
MAXIMUM = 0.4507

MINIMUM = 0.1000
MAXIMUM = 0.5000

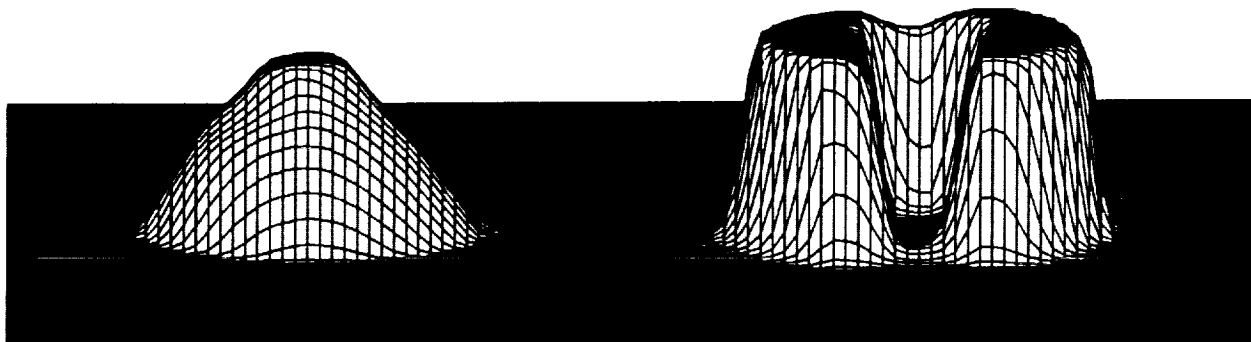


FIGURE 23. - 1 ROTATION - SUPERBEE INTERPOLATION.

MINIMUM = 0.1000
MAXIMUM = 0.4974

MINIMUM = 0.0890
MAXIMUM = 0.5675

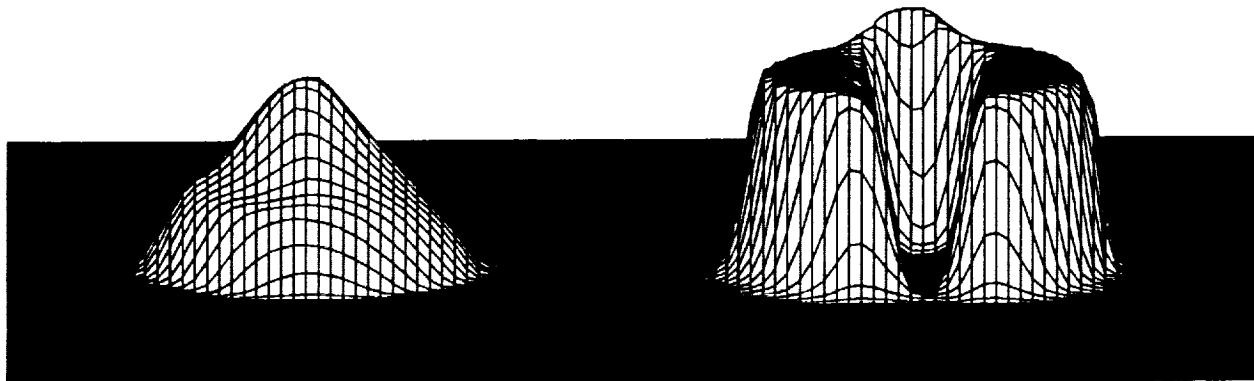


FIGURE 24. - 1 ROTATION - SONIC B INTERPOLATION.

ORIGINAL PAGE
BLACK AND WHITE PHOTOGRAPH

MINIMUM = 0.1000
MAXIMUM = 0.4412

MINIMUM = 0.0875
MAXIMUM = 0.5021

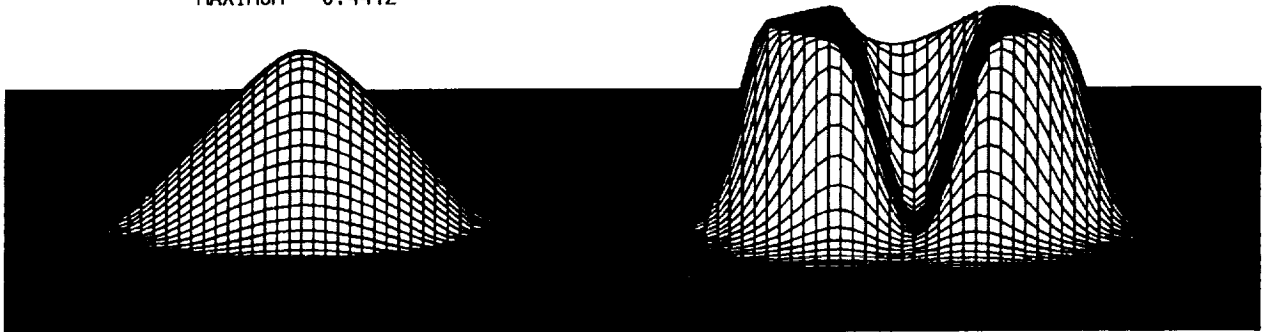


FIGURE 25. - 1 ROTATION - SONIC A INTERPOLATION.

MINIMUM = 0.1000
MAXIMUM = 0.2527

MINIMUM = 0.1000
MAXIMUM = 0.3244

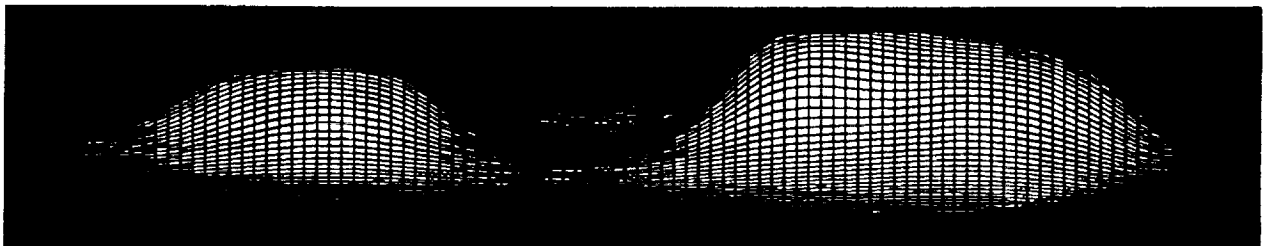


FIGURE 26. - 6 ROTATIONS - MINMOD INTERPOLATION.

MINIMUM = 0.1000
MAXIMUM = 0.4498

MINIMUM = 0.1000
MAXIMUM = 0.5000

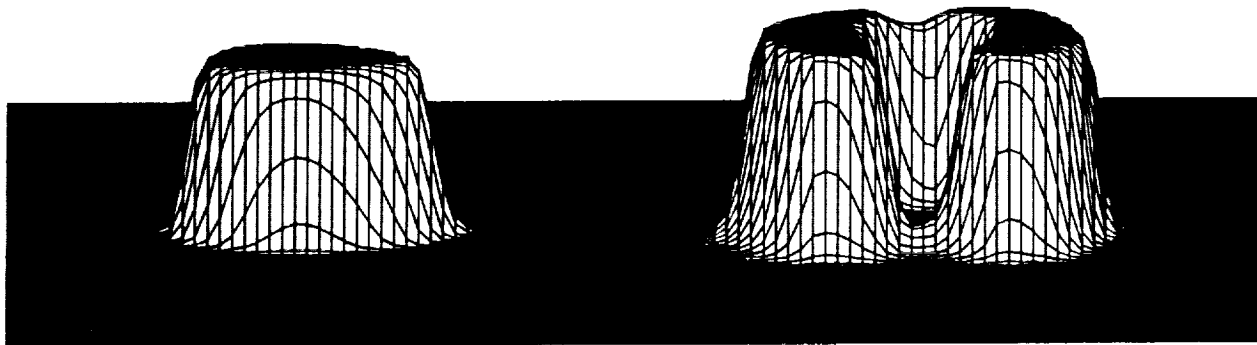


FIGURE 27. - 6 ROTATIONS - SUPERBEE INTERPOLATION.

MINIMUM = 0.1000
MAXIMUM = 0.5016

MINIMUM = -.0216
MAXIMUM = 0.5331

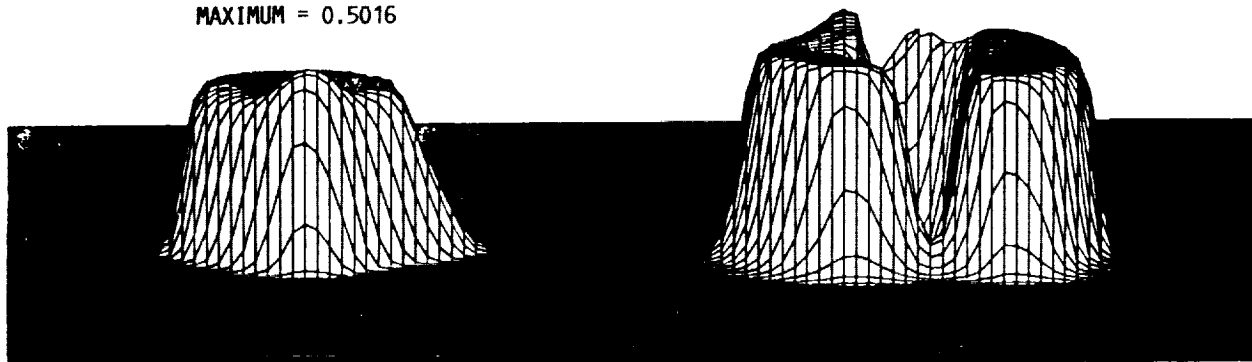


FIGURE 28. - 6 ROTATIONS - SONIC B INTERPOLATION.

MINIMUM = 0.1000
MAXIMUM = 0.3726

MINIMUM = 0.1000
MAXIMUM = 0.5046

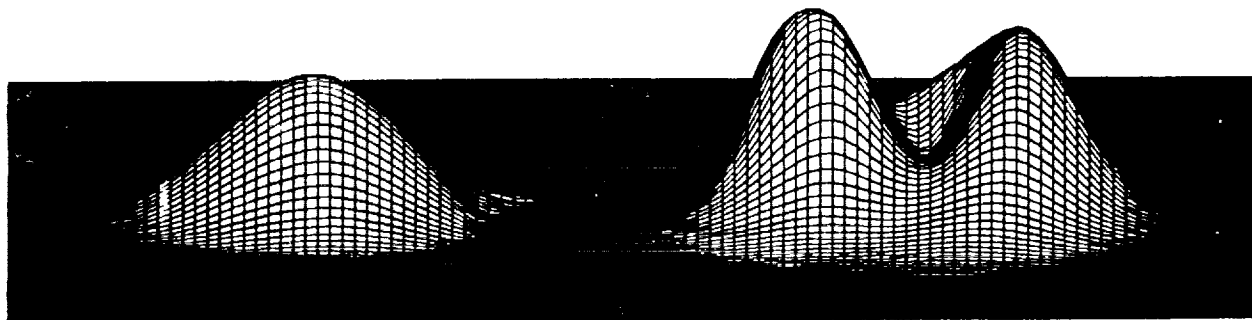


FIGURE 29. - 6 ROTATIONS - SONIC A INTERPOLATION.



Report Documentation Page

1. Report No. NASA TM-102354	2. Government Accession No.	3. Recipient's Catalog No.	
4. Title and Subtitle A Nonoscillatory, Characteristically Convected, Finite Volume Scheme for Multidimensional Convection Problems		5. Report Date	
		6. Performing Organization Code	
7. Author(s) Jeffrey W. Yokota and Hung T. Huynh		8. Performing Organization Report No. E-5069	
		10. Work Unit No. 505-62-21	
9. Performing Organization Name and Address National Aeronautics and Space Administration Lewis Research Center Cleveland, Ohio 44135-3191		11. Contract or Grant No.	
		13. Type of Report and Period Covered Technical Memorandum	
12. Sponsoring Agency Name and Address National Aeronautics and Space Administration Washington, D.C. 20546-0001		14. Sponsoring Agency Code	
		15. Supplementary Notes Prepared for the 28th Aerospace Sciences Meeting sponsored by the American Institute of Aeronautics and Astronautics, Reno, Nevada, January 8-11, 1990. Jeffrey W. Yokota, Sverdrup Technology, Inc., NASA Lewis Research Center Group, Cleveland, Ohio 44135; Hung T. Huynh, NASA Lewis Research Center.	
16. Abstract A new, nonoscillatory upwind scheme is developed for the multidimensional convection equation. The scheme consists of an upwind, nonoscillatory interpolation of data to the surfaces of an intermediate finite volume; a characteristic convection of surface data to a midpoint time level; and a conservative time integration based on the midpoint rule. This procedure results in a convection scheme capable of resolving discontinuities neither aligned with, nor convected along, grid lines.			
17. Key Words (Suggested by Author(s)) Nonoscillatory Upwind Multidimensional convection		18. Distribution Statement Unclassified - Unlimited Subject Category 64	
19. Security Classif. (of this report) Unclassified	20. Security Classif. (of this page) Unclassified	21. No of pages 18	22. Price* A03

